

## Supporting Information

### **Solar energy-driven electrolysis with molecular catalysts for reduction of carbon dioxide coupled with oxidation of 5- hydroxymethylfurfural**

Zhi-Wen Yang, Jin-Mei Chen, Li-Qi Qiu, Wen-Jun Xie, and Liang-Nian He\*

*State Key Laboratory and Institute of Elemento-Organic Chemistry, College of Chemistry, Nankai  
University, Tianjin 300071, P. R. China.*

# Catalogue

<b>1. Experimental details</b> .....	S3
1.1 Materials and reagents.....	S3
1.2 Instrumentation and characterizations.....	S3
1.3 Catalysts synthesis and electrode preparation.....	S4
1.4 Electrochemical measurements.....	S6
1.5 Product analysis.....	S7
1.6 DFT calculation details.....	S8
<b>2. Supplementary figures and tables</b> .....	S8
Fig. S1 <sup>1</sup> H NMR spectrum of TBP-PN.....	S8
Fig. S2 <sup>13</sup> C NMR spectrum of TBP-PN.....	S9
Fig. S3 MALDI-HRMS of TBP-CoPc.....	S9
Fig. S4 FT-IR spectra of TBP-CoPc and TBP-PN.....	S10
Fig. S5 The optical photographs of TBP-CoPc and CoPc in DMF.....	S10
Fig. S6 UV-Vis spectra of TBP-CoPc and CoPc.....	S11
Fig. S7 Energy levels of HOMO and LUMO of TBP-CoPc and CoPc.....	S11
Fig. S8 SEM and energy dispersive X-ray spectroscopy of TBP-CoPc/CNTs.....	S12
Fig. S9 UV-Vis spectra of TBP-CoPc/CNTs, CNTs and TBP-CoPc.....	S12
Fig. S10 X-ray crystal structure of Py-TEMPO catalyst.....	S13
Table S1 Crystal data and structure refinement for Py-TEMPO.....	S14
Table S2 Bond lengths for Py-TEMPO.....	S15
Table S3 Bond angles for Py-TEMPO.....	S16
Fig. S11 CV curves of Py-TEMPO/CNTs at varying pH.....	S17
Fig. S12 Gas product analysis.....	S17
Fig. S13 <sup>1</sup> H NMR spectra of the liquid product for ECO <sub>2</sub> RR.....	S18
Fig. S14 <sup>1</sup> H NMR spectra of possible product for HMFOR.....	S18
Fig. S15 I-t curves of CO <sub>2</sub> RR with TBP-CoPc/CNTs at different potentials.....	S19
Fig. S16 The optical photograph at the anodic part of H-cell after CPE for HMFOR at 1.0 V.....	S19
Fig. S17 <sup>1</sup> H NMR spectrum of anolyte after CPE for HMFOR at 1.0 V.....	S20
Fig. S18 Product distribution in the sun-light-driven paired electrolysis.....	S20
<b>3. Reference</b> .....	S20

# 1. Experimental details

## 1.1 Materials and reagents

Carbon dioxide (purity 99.999%) and Ar (purity 99.999%) were used. All the organic solvents used for reactions were distilled under argon after drying over an appropriate drying agent. The  $\text{KHCO}_3$  solution used for  $\text{ECO}_2\text{RR}$  has been pretreated with Chelex 100 resin before electrolysis to get rid of other potential trace metal ions and keep away from impurity metal deposition. Multi-walled carbon nanotubes (MWCNTs, inner diameter: 5-10 nm; outer diameter: 10-20 nm; length: 10-30  $\mu\text{m}$ ) were calcined in muffle furnace at 500  $^\circ\text{C}$  for 5 h, which were then transferred into 5 wt% HCl aqueous solution after being cooled down to room temperature and sonicated for 30 min. The CNTs were subsequently filtered and washed with deionized water, which was then lyophilized. The carbon paper (Ce-tech NOS1005) and carbon cloth (Ce-tech WOS1009) were pretreated with 2 M nitric acid and acetone. Unless otherwise stated, other reagents were purchased from commercial sources and used without further treatment.

## 1.2 Instrumentation and characterizations

$^1\text{H}$  NMR and  $^{13}\text{C}$  NMR spectra were recorded on a Bruker 400 MHz spectrometer with residual solvent peaks used as the internal reference. Fourier transform infrared (FT-IR) spectra were recorded on a Bruker Tensor 27 FT-IR spectrophotometer with KBr pellets. UV-Vis spectra were recorded on a Varian Cary 300 Conc spectrophotometer. High resolution mass spectrometry (HRMS) analysis was performed on Varian 7.0T spectrometer by electrospray ionization (ESI) technique or Bruker Solarix scimax spectrometer by matrix assisted laser desorption ionization (MALDI) technique. The metal contents of the catalysts were analyzed using inductively coupled plasma-optical emission spectrometry (ICP-OES) on SpectroBlue. Scanning electron microscopy (SEM) was characterized on ZEISS MERLIN Compact. Elemental analysis were measured by vario EL CUBE elemental analyzer. Single-crystal structure was attained through Rigaku 007 Saturn 70 X-ray single crystal diffractometer (Mo target). All the electrochemical tests were performed with CHI 660E electrochemical workstation. The potential not controlled by the electrochemical workstation during coupled electrolysis was determined by DT9205A<sup>+</sup> type multimeter. Analysis of gas product was conducted on gas chromatograph FULI 9790 equipped with thermal conductivity detector (TCD) using Ar as carrier gas.

### 1.3 Catalysts synthesis and electrode preparation

#### 1.3.1 Synthesis of 4-(4-(tert-butyl)phenoxy)phthalonitrile (TBP-PN)

The procedure is according to the literature with some modification.<sup>1</sup> 4-nitrophthalonitrile (1000 mg, 5.78 mmol), 4-tert-butylphenol (1379 mg, 9.18 mmol) and K<sub>2</sub>CO<sub>3</sub> (2500 mg, 18.08 mmol) in DMF (20 mL) were stirred at room temperature under Ar for 24 h. Subsequently, the mixture was poured into 200 mL distilled water and white solid participated, which was then filtered and washed with water. After that, the white solid was dried at 80 °C in vacuum for 12 h and then purified by silicone gel column chromatography with CH<sub>2</sub>Cl<sub>2</sub> as the eluents, giving white solid 1427.6 mg (yield 89.4%). Melt Point: 117–119 °C. <sup>1</sup>H NMR (400 MHz, DMSO-*d*<sub>6</sub>): δ (ppm) 8.08 (d, *J* = 8.8 Hz, 1H), 7.77 (d, *J* = 2.3 Hz, 1H), 7.51 (d, *J* = 8.6 Hz, 2H), 7.33 (dd, *J* = 8.8, 2.3 Hz, 1H), 7.12 (d, *J* = 8.6 Hz, 2H), 1.30 (s, 9H). <sup>13</sup>C NMR (100 MHz, DMSO-*d*<sub>6</sub>): δ (ppm) 161.3, 151.3, 148.2, 136.3, 127.3, 122.4, 121.6, 119.8, 116.6, 115.9, 115.3, 107.9, 34.2, 31.1. FT-IR (KBr, ν/cm<sup>-1</sup>): 3083, 3055, 2961, 2868, 2230, 1586, 1481, 1243, 1019. HRMS (ESI): *m/z*, [M+H]<sup>+</sup> cal. 277.1341, found 277.1333.

#### 1.3.2 Synthesis of tetra-(4-(tert-butyl)phenoxy) cobalt phthalocyanine (TBP-CoPc)

The procedure is according to the literature with some modification.<sup>2</sup> TBP-PN (1105.4 mg, 4 mmol), CoCl<sub>2</sub> (142.8 mg, 1.1 mmol) and 4 mL DBU (1,8-diazabicyclo[5.4.0]undec-7-ene) in 10 mL pentanol were stirred at 140 °C for 12 h under Ar. The black mixture was poured into 100 mL methanol and then the solid was filtered and washed with methanol. Subsequently, the product was purified by silica gel column chromatography (CH<sub>2</sub>Cl<sub>2</sub>/acetone = 10/1, V/V) to give blue purple solid 130.9 mg (yield 11.2%). HRMS (MALDI): *m/z*, [M+H]<sup>+</sup> cal. 1164.4461, found 1164.4436. Elem. Anal. (%): cal. C, 74.28; H, 5.54; N, 9.62; found (%) C, 73.79; H, 5.59; N, 9.33. FT-IR (KBr, ν/cm<sup>-1</sup>): 3062, 3037, 2960, 2903, 2867, 1602, 1524, 1472, 1363, 1332, 1268, 1238, 1167, 1120, 1058, 1014, 958, 879, 827, 753.

#### 1.3.3 Synthesis of Py-TEMPO

This catalysts was synthesized according to the literature method with slight modification.<sup>3</sup> Pyrene-1-butyric acid (288.3 mg, 1 mmol) and 4-amino-TEMPO (171.3 mg, 1 mmol) were weighed into a 100 mL two-necked flask under Ar, which were than dissolved in 20 mL dried CH<sub>2</sub>Cl<sub>2</sub> and stirred at room temperature for 30 min. Subsequently, 4-dimethylamino pyridine (12.2

mg, 0.1 mmol) and *N,N'*-Dicyclohexylcarbodiimide (206.3 mg, 1 mmol) were added into the flask under Ar and the mixture was stirred at room temperature for 24 h. Subsequently, the reaction mixture was filtered and the filtrate was evaporated under vacuum to obtain the crude product, which was then purified by silica gel column chromatography (hexane/ethyl = 3/7, V/V). The obtained orange oil was dissolved in CH<sub>2</sub>Cl<sub>2</sub> and then excess hexane was added. Then orange red solid precipitated and was dried under vacuum after filtering, obtaining 245.1 mg product (yield 55.5%). HRMS (ESI): *m/z*, [M+H]<sup>+</sup> cal. 464.2435, found 464.2435. FT-IR (KBr, ν/cm<sup>-1</sup>): 3322, 3037, 2993, 2861, 1640, 1541, 839. Recrystallization of the solid by slow diffusion of hexanes into saturated CH<sub>2</sub>Cl<sub>2</sub> solution gave an orange red crystal suitable for crystallography.

#### *1.3.4 Synthesis of TBP-CoPc/CNTs*

3 mg TBP-CoPc was dissolved in 20 mL DMF initially. 60 mg MWCNTs was added into 40 mL DMF and the mixture was sonicated for 1 h to disperse the MWCNTs. Subsequently, the above solutions were mixed and sonicated for 0.5 h. which was then stirred at room temperature for 24 h. The suspension was centrifuged and the black precipitate was washed with DMF and water. Finally, the solid was lyophilized to yield the final product 53.6 mg. The weight percentage of cobalt in the TBP-CoPc/CNTs was measured as 0.201 wt% by ICP-OES test.

#### *1.3.5 Preparation of electrode for ECO<sub>2</sub>RR*

2.0 mg TBP-CoPc/CNTs was added into a mixture of 170 μL 0.5 wt% Nafion solution and 830 μL ethanol. Then the suspension was sonicated for 1 h to promote the dispersion. 100 μL of the catalyst ink was drop-coated on a 1 x 1 cm<sup>2</sup> carbon paper, which was then dried by heating at 100 °C. The electrodes of 2 cm<sup>2</sup> and 4 cm<sup>2</sup> were prepared by drop-coating 200 μL and 400 μL catalyst ink on 1 x 2 cm<sup>2</sup> and 2 x 2 cm<sup>2</sup> carbon paper, respectively. It is worth mentioning that default 1 x 1 cm<sup>2</sup> cathode was used in the di-electrode electrolysis and solar-driven paired electrolysis experiments.

#### *1.3.6 Preparation of electrode for HMFOR*

5 mg MWCNTs and 2 mg carbon nanofiber were dispersed in 1400 μL ethanol solution of Py-TEMPO (5 mM) with sonication for 1 h. 700 μL of the catalyst ink was drop-coated on a 1.5 x 3 cm<sup>2</sup> carbon cloth, which was then dried by heating at 100 °C.

## 1.4 Electrochemical measurements

Electrochemical experiments were performed using CHI 660E electrochemical working station and a commercial gas-tight two-compartment cell. The two compartments of the cell were separated by N117 proton exchange membrane. In the linear sweep voltammetry and cyclic voltammetry tests for the characterization of the catalysts, the potentials were  $iR$  corrected at 95% level. The Ohmic drop  $R$  was measured by electrochemical impedance spectroscopy (EIS) at open circuit potential between 100 kHz and 0.1 Hz with an amplitude of 5 mV. In order to simulate more practical system and compare the potential-product relationship between the paired and individual electrolysis more intuitively, the potentials in these constant potential electrolysis (CPE) tests were without  $iR$  correction.

### 1.4.1 Individual $CO_2RR$ experiment.

20 mL 0.1 M  $KHCO_3$  aqueous solution was used as the electrolyte in both parts of the H-Cell. Before electrolysis, the electrolyte of cathodic zone was pre-saturated with  $CO_2$  through bubbling the gas for 30 min and then sealed. Graphite rod and saturated Ag/AgCl electrode were used as counter electrode and reference electrode, respectively.

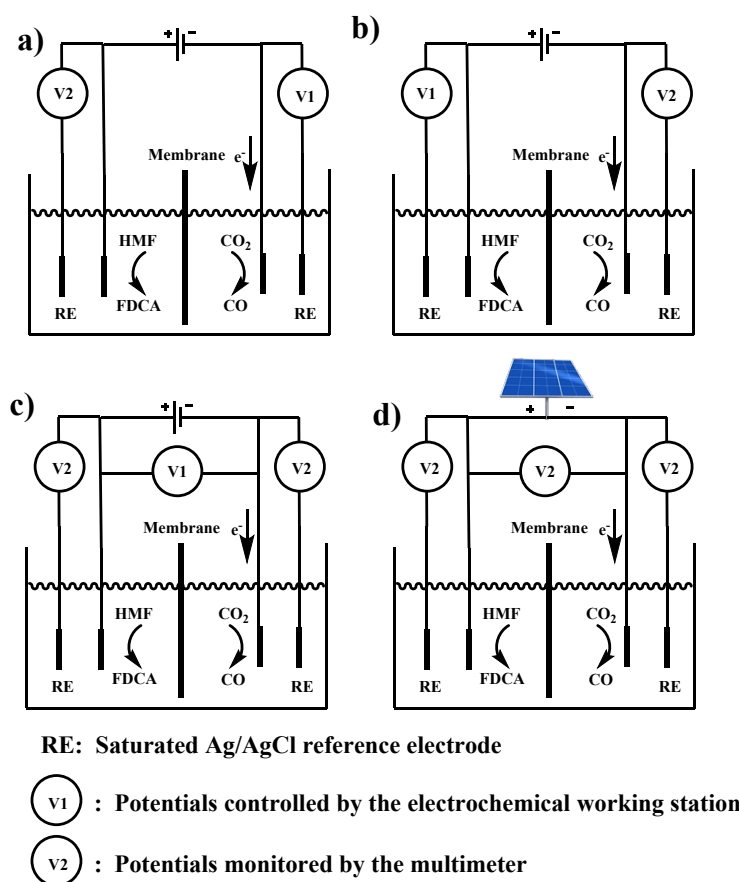
### 1.4.2 Individual HMFOR experiment.

20 mL 0.1 M  $KHCO_3$  aqueous solution was used as catholyte. 20 mL 0.2 M  $Na_2CO_3$  and 5 mM HMF aqueous solution were used as anolyte. Platinum foil (1 x 1 cm<sup>2</sup>) and saturated Ag/AgCl electrode were used as counter electrode and reference electrode, respectively. The electrolysis was halted when 57.9 C charge (stoichiometric charge for full transformation of HMF to FDCA) passed or the current decreased to < 0.1 mA.

### 1.4.3 Paired electrolysis

20 mL 0.1 M  $KHCO_3$  aqueous solution was used as catholyte. Before electrolysis, the electrolyte of cathodic zone was pre-saturated with  $CO_2$  through bubbling the gas for 30 min and then sealed. 20 mL 0.2 M  $Na_2CO_3$  and 5 mM HMF aqueous solution were used as anolyte. The electrolysis was halted when 57.9 C charge passed. The potentials not controlled by the electrochemical workstation during coupled electrolysis were determined by multimeter. The sunlight-driven paired electrolysis was conducted under similar condition with a commercial solar panel in replacement of electrochemical workstation. The detailed device structure is illustrated in

Scheme S1.



**Scheme S1.** Schematic illustration for the device structure for paired electrolysis. a) Tri-electrode system with potential of CO<sub>2</sub>RR controlled. b) Tri-electrode system with potential of HMFOR controlled. c) Di-electrode system with cell voltage controlled. d) Sun-light-driven paired electrolysis.

## 1.5 Product analysis

After the electrolysis, 1 mL gas sample from the headspace of the cathodic part was drawn by gas-tight syringes and analyzed by gas chromatography. The product in the liquid phase was analyzed by <sup>1</sup>H NMR with DMSO as internal standard: 392 μL electrolyte sample was mixed with 48 μL D<sub>2</sub>O and 40 μL DMSO aqueous solution (4.022 mM), which was tested by 128 scans accumulated with pre-saturation technique in <sup>1</sup>H NMR.

Faradaic efficiency for the gas product in ECO<sub>2</sub>RR is calculated as following:

$$FE = \frac{PV\psi(CO)}{RT} \times \frac{NF}{Q} \times 100\% \dots\dots\dots(1)$$

P is atmospheric pressure (101325 Pa); V is the volume of the space over electrolyte in the cathodic part (43.5 × 10<sup>-6</sup> m<sup>3</sup>); ψ(CO) is the volume fraction of CO in the gas sample, which is

determined by gas chromatography with calibration curves (Figure S12); R is the ideal gas constant ( $8.314 \text{ J mol}^{-1} \text{ K}^{-1}$ ); T is the room temperature (298.15 K); N is the moles of electrons for obtaining per mole product, which equals 2 for CO and H<sub>2</sub>; F is the Faradaic constant ( $96485 \text{ C mol}^{-1}$ ), Q is the total charge flowing through the electrode surface (C).

Faradaic efficiency for the liquid product in ECO<sub>2</sub>RR and HMFOR is calculated as following:

$$\text{FE} = \frac{nNF}{Q} \times 100\% \dots\dots\dots(1)$$

n is the amount of produced liquid product calculated from <sup>1</sup>H NMR with DMSO as internal standard (mol). N is the moles of electrons for producing per mole product, which equals 6 for reducing CO<sub>2</sub> to CH<sub>3</sub>OH and oxidizing HMF to FDCA, 4 for oxidizing HMF to FFCA; Q is the total charge flowing through the electrode surface (C).

### 1.6 DFT calculation details

The DFT calculations were performed using Gaussian 09 (Revision D.01)<sup>4</sup> at the PBE0/6-31G(d) level. The Lan12dz basis for Co atom and 6-31G(d) basis for other atoms. The D3(BJ) empirical dispersion correction was considered to make the results more accurate.

## 2. Supplementary figures and tables

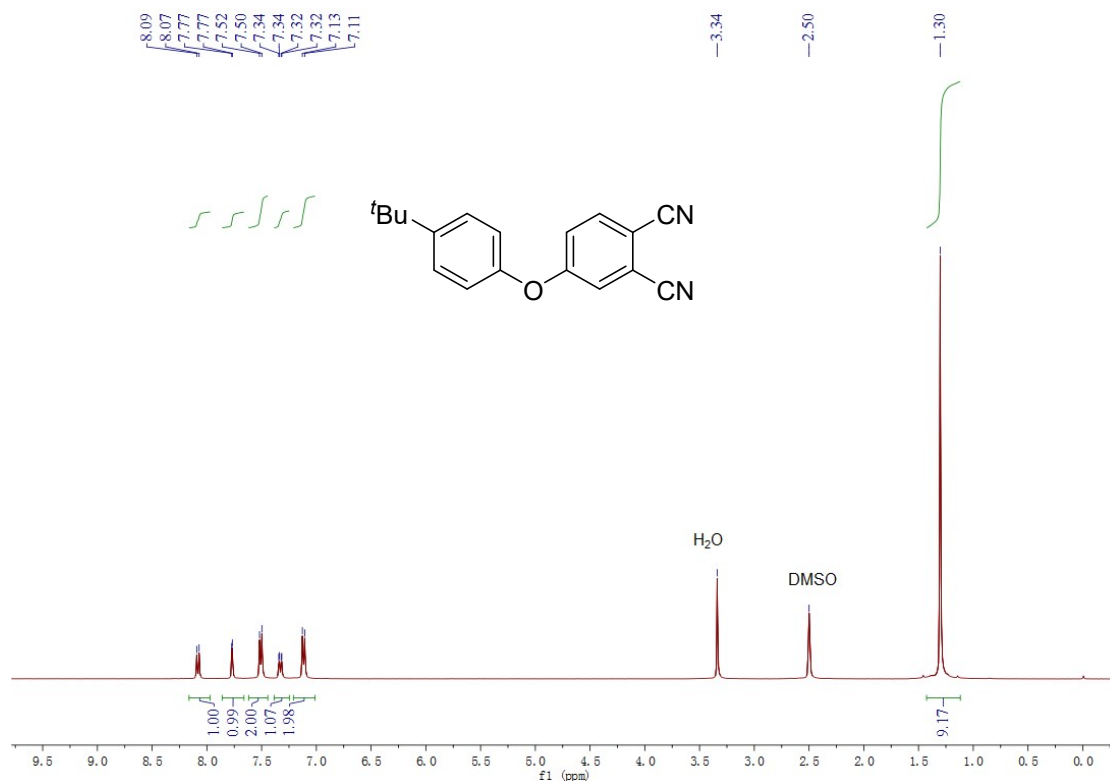


**Fig. S1**  $^1\text{H}$  NMR spectrum of TBP-PN (400 MHz,  $\text{DMSO-}d_6$ ).

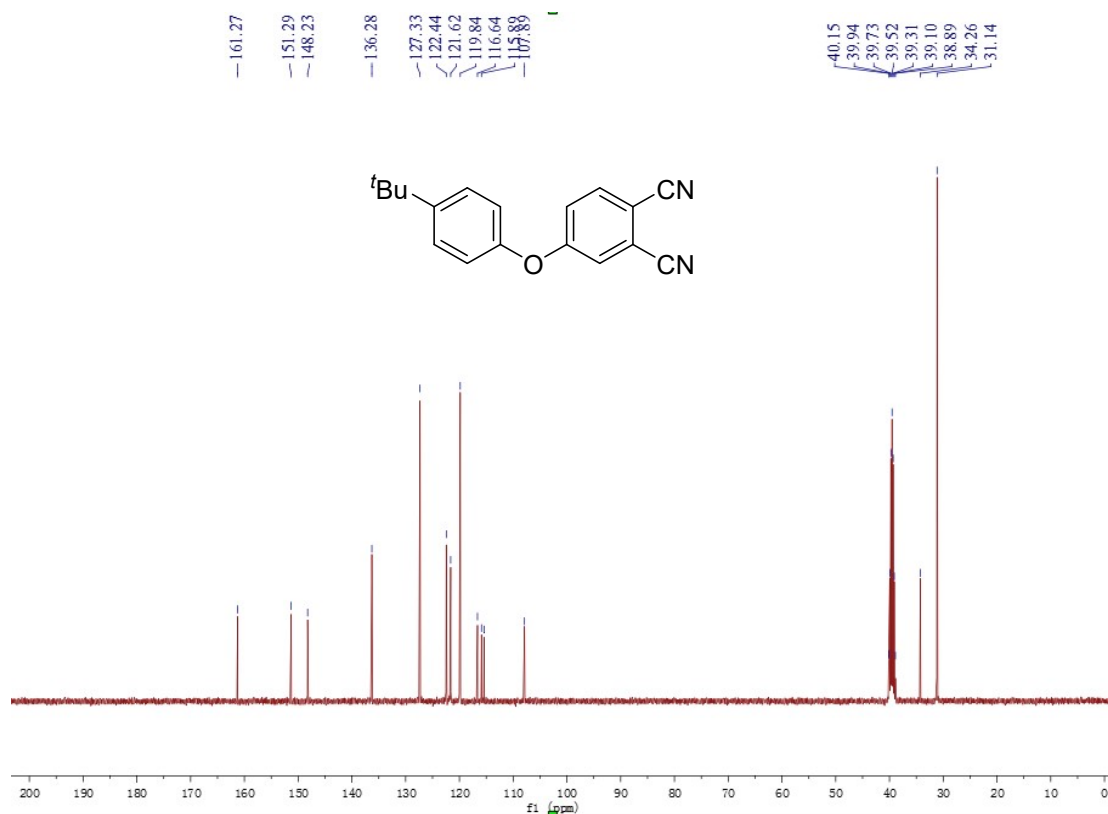


**Fig. S2**  $^{13}\text{C}$  NMR spectrum of TBP-PN (101 MHz,  $\text{DMSO-}d_6$ ).

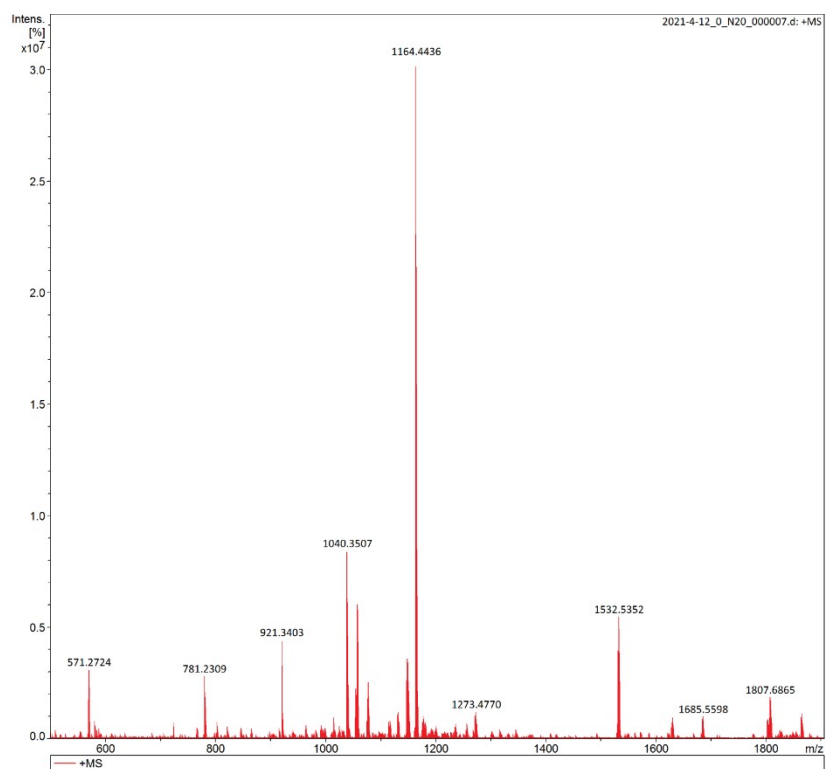


**Fig. S3** MALDI-HRMS of TBP-CoPc.

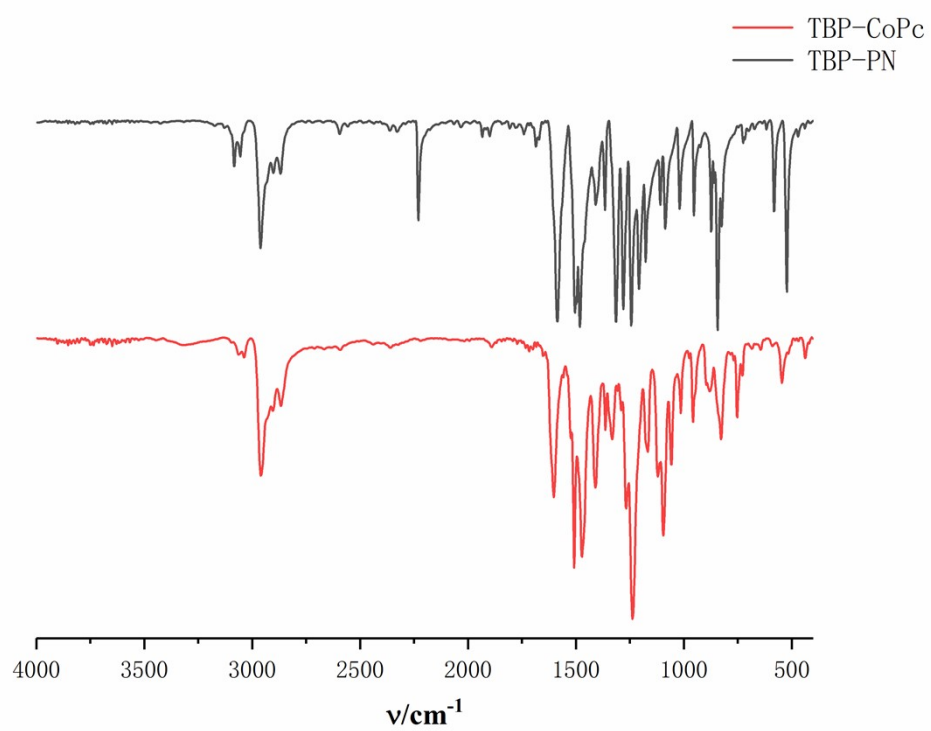


**Fig. S4** FT-IR spectra of TBP-CoPc and TBP-PN (KBr,  $\text{cm}^{-1}$ ).

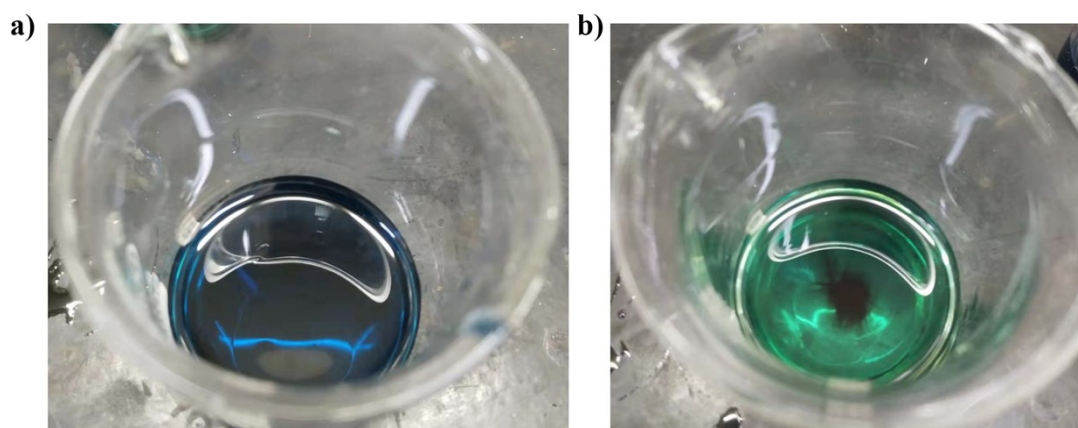


**Fig. S5** The optical photographs of a) TBP-CoPc and b) CoPc in DMF (1.5 mg in 10 mL DMF).

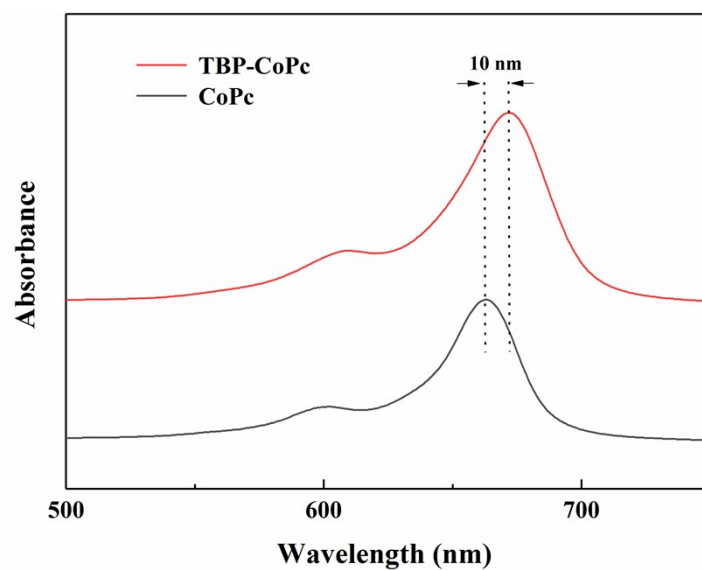


**Fig. S6** UV-Vis spectra of TBP-CoPc and CoPc ( $1 \times 10^{-5}$  M in DMF).

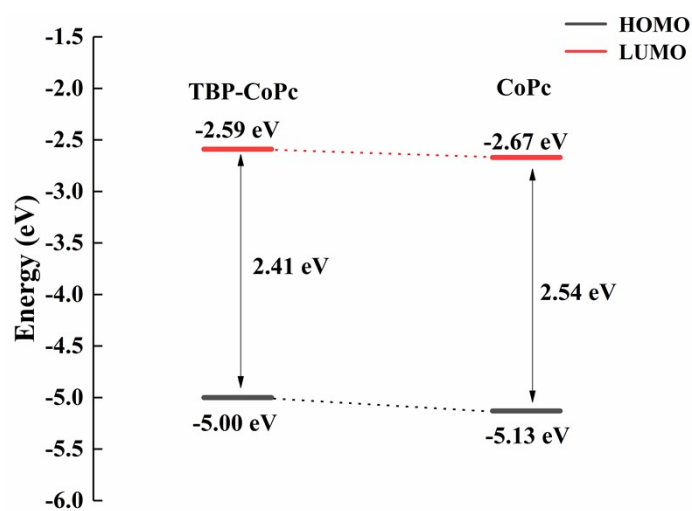


**Fig. S7** Energy levels of HOMO and LUMO of TBP-CoPc and CoPc from DFT calculation.

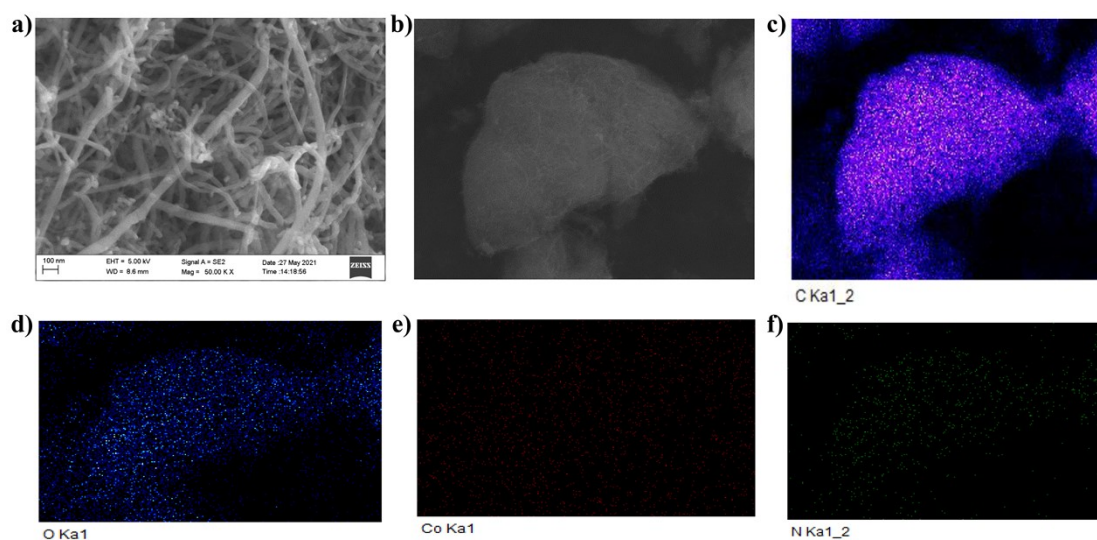


**Fig. S8** a-b) SEM and (c-f) corresponding energy dispersive X-ray spectroscopy of TBP-CoPc/CNTs.

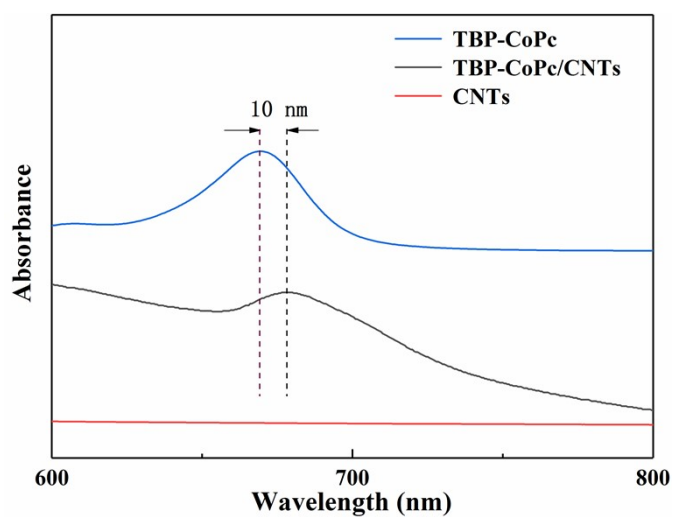


**Fig. S9** UV-Vis spectra of TBP-CoPc/CNTs, CNTs and TBP-CoPc ( $C_{\text{CNTs, TBP-CoPc-CNTs}} = 0.05 \text{ mg mL}^{-1}$ ,  $C_{\text{TBP-CoPc}} = 1 \times 10^{-5} \text{ mol L}^{-1}$ ).

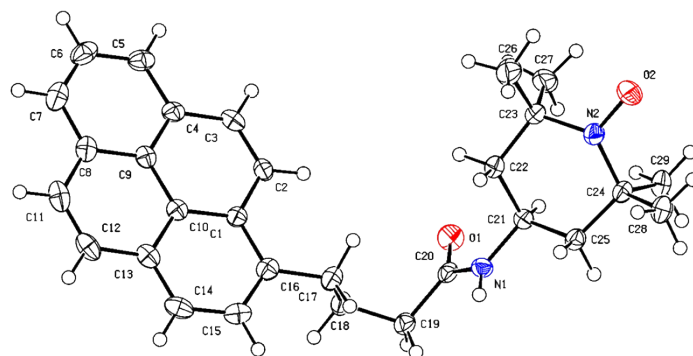


**Fig. S10** X-ray crystal structure of Py-TEMPO catalyst. CCDC reference number: 2133378.

**Table S1** Crystal data and structure refinement for Py-TEMPO.

Identification code	Py-TEMPO
Empirical formula	C <sub>29</sub> H <sub>33</sub> N <sub>2</sub> O <sub>2</sub>
Formula weight	441.57
Temperature (K)	113.15
Crystal system	monoclinic
Space group	P2 <sub>1</sub> /c
a (Å)	20.6047(9)
b (Å)	11.4378(5)
c (Å)	10.1417(5)
α (°)	90
β (°)	92.408(4)
γ (°)	90
Volume (Å <sup>3</sup> )	2388.01(19)
Z	4
ρ <sub>calc</sub> (g cm <sup>-3</sup> )	1.228
μ (mm <sup>-1</sup> )	0.077
F(000)	948.0
Crystal size (mm <sup>3</sup> )	0.22 × 0.2 × 0.16
Radiation	MoKα (λ = 0.71073)
2θ range for data collection (°)	3.956 to 56.562
Index ranges	-27 ≤ h ≤ 27, -15 ≤ k ≤ 15, -13 ≤ l ≤ 13
Reflections collected	8054
Independent reflections	8054 [R <sub>int</sub> = ?, R <sub>sigma</sub> = 0.0419]
Data/restraints/parameters	8054/0/304
Goodness-of-fit on F <sup>2</sup>	1.018
Final R indexes [I ≥ 2σ (I)]	R <sub>1</sub> = 0.0649, wR <sub>2</sub> = 0.1663
Final R indexes [all data]	R <sub>1</sub> = 0.0873, wR <sub>2</sub> = 0.1760
Largest diff. peak/hole (e Å <sup>-3</sup> )	0.30/-0.25

**Table S2** Bond lengths for Py-TEMPO.

<b>Atom</b>	<b>Atom</b>	<b>Length/Å</b>	<b>Atom</b>	<b>Atom</b>	<b>Length/Å</b>
O1	C20	1.233(3)	C10	C13	1.425(3)
O2	N2	1.283(2)	C11	C12	1.338(4)
N1	C20	1.344(3)	C12	C13	1.437(3)
N1	C21	1.455(3)	C13	C14	1.383(3)
N2	C23	1.496(3)	C14	C15	1.384(4)
N2	C24	1.496(3)	C15	C16	1.389(3)
C1	C2	1.440(3)	C16	C17	1.509(3)
C1	C10	1.421(3)	C17	C18	1.529(3)
C1	C16	1.412(3)	C18	C19	1.527(3)
C2	C3	1.346(3)	C19	C20	1.511(3)
C3	C4	1.434(3)	C21	C22	1.523(3)
C4	C5	1.403(3)	C21	C25	1.518(3)
C4	C9	1.415(3)	C22	C23	1.526(3)
C5	C6	1.380(3)	C23	C26	1.525(3)
C6	C7	1.377(4)	C23	C27	1.530(3)
C7	C8	1.394(3)	C24	C25	1.525(3)
C8	C9	1.429(3)	C24	C28	1.529(3)
C8	C11	1.434(3)	C24	C29	1.531(3)
C9	C10	1.420(3)			

**Table S3** Bond angles for Py-TEMPO.

Atom	Atom	Atom	Angle/°	Atom	Atom	Atom	Angle/°
C20	N1	C21	122.12(18)	C13	C14	C15	120.8(2)
O2	N2	C23	115.79(17)	C14	C15	C16	122.0(2)
O2	N2	C24	115.41(17)	C1	C16	C17	122.3(2)
C24	N2	C23	124.47(17)	C15	C16	C1	118.8(2)
C10	C1	C2	117.96(19)	C15	C16	C17	118.9(2)
C16	C1	C2	122.6(2)	C16	C17	C18	113.57(18)
C16	C1	C10	119.4(2)	C19	C18	C17	112.17(18)
C3	C2	C1	121.5(2)	C20	C19	C18	112.21(18)
C2	C3	C4	121.2(2)	O1	C20	N1	122.6(2)
C5	C4	C3	122.0(2)	O1	C20	C19	121.6(2)
C5	C4	C9	119.1(2)	N1	C20	C19	115.76(19)
C9	C4	C3	118.95(19)	N1	C21	C22	110.93(18)
C6	C5	C4	120.5(2)	N1	C21	C25	109.81(17)
C7	C6	C5	120.9(2)	C25	C21	C22	108.13(18)
C6	C7	C8	121.1(2)	C21	C22	C23	113.38(18)
C7	C8	C9	118.7(2)	N2	C23	C22	109.88(18)
C7	C8	C11	123.1(2)	N2	C23	C26	107.3(2)
C9	C8	C11	118.2(2)	N2	C23	C27	109.15(19)
C4	C9	C8	119.7(2)	C22	C23	C27	111.6(2)
C4	C9	C10	119.7(2)	C26	C23	C22	109.0(2)
C10	C9	C8	120.6(2)	C26	C23	C27	109.8(2)
C1	C10	C13	120.1(2)	N2	C24	C25	110.20(17)
C9	C10	C1	120.5(2)	N2	C24	C28	107.56(18)
C9	C10	C13	119.4(2)	N2	C24	C29	108.77(18)
C12	C11	C8	121.2(2)	C25	C24	C28	109.10(18)
C11	C12	C13	122.1(2)	C25	C24	C29	111.72(19)
C10	C13	C12	118.4(2)	C28	C24	C29	109.39(19)
C14	C13	C10	118.8(2)	C21	C25	C24	113.77(17)
C14	C13	C12	122.8(2)				

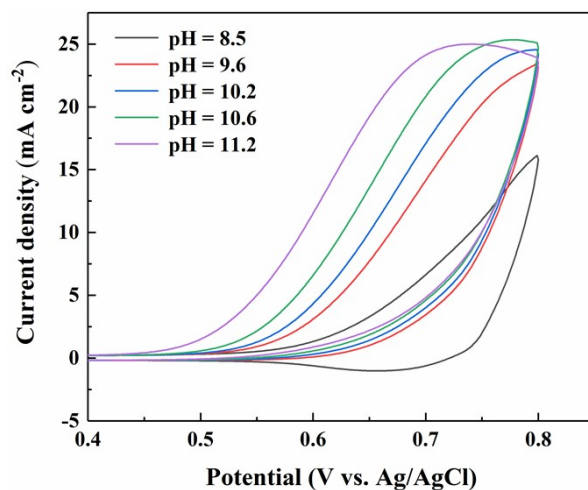


**Fig. S11** CV curves of Py-TEMPO/CNTs at varying pH conditions from 8.5 to 11.2 with 5 mM HMF in the 0.2 M carbonate aqueous solution. The pH value is controlled by the ratio of Na<sub>2</sub>CO<sub>3</sub>/NaHCO<sub>3</sub>. Scan rate: 100 mV s<sup>-1</sup>.

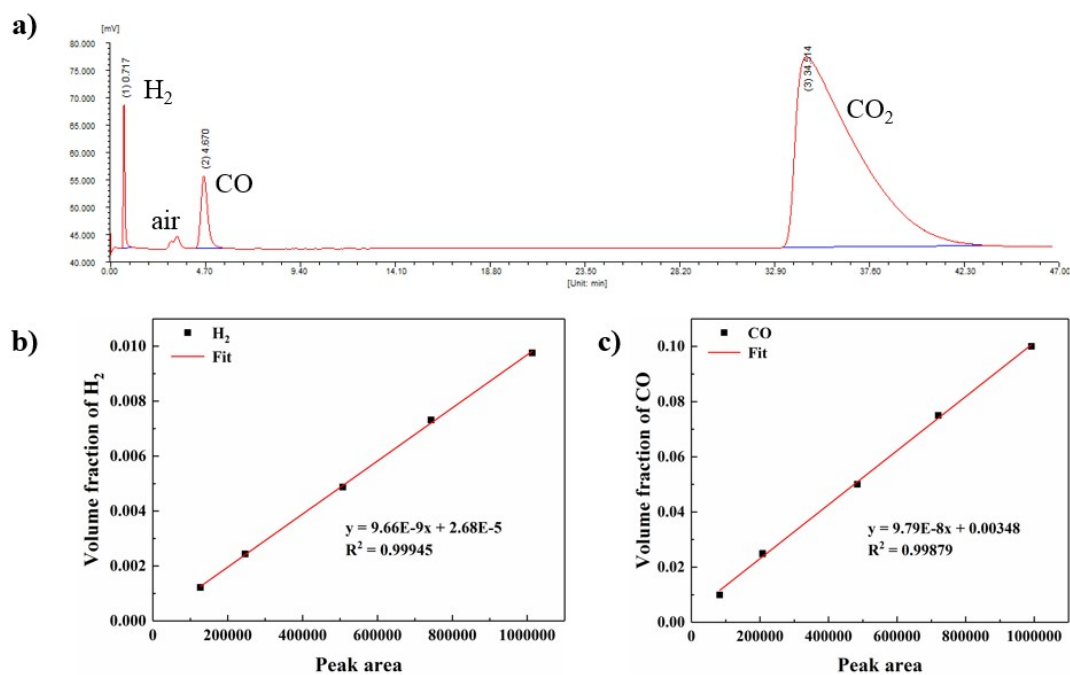


**Fig. S12** Gas products analysis. a) Gas chromatogram of the gas product. b) Calibration curves for H<sub>2</sub> and CO detected by GC-TCD.

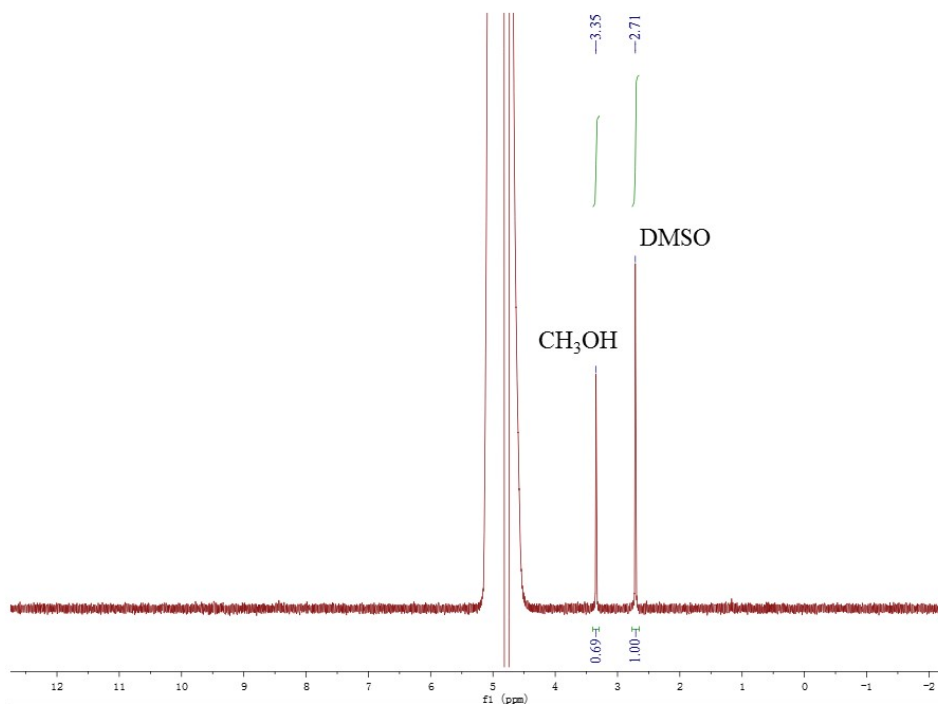


**Fig. S13**  $^1\text{H}$  NMR spectra of the liquid product for  $\text{ECO}_2\text{RR}$  (400 MHz,  $\text{D}_2\text{O}:\text{H}_2\text{O} = 1:9$ ).

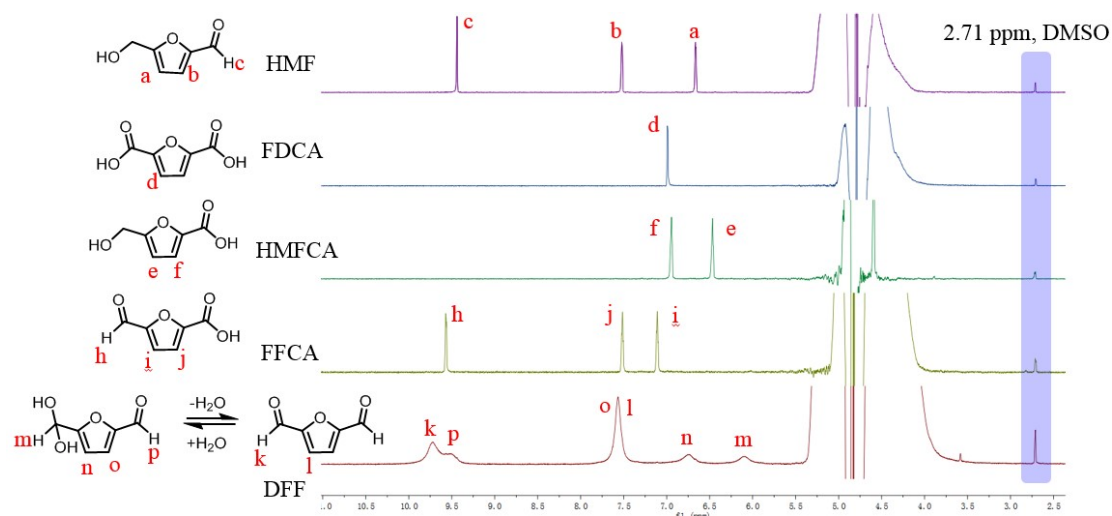


**Fig. S14**  $^1\text{H}$  NMR spectra of possible products for HMFOR (400 MHz,  $\text{D}_2\text{O}:\text{H}_2\text{O} = 1:9$ ).

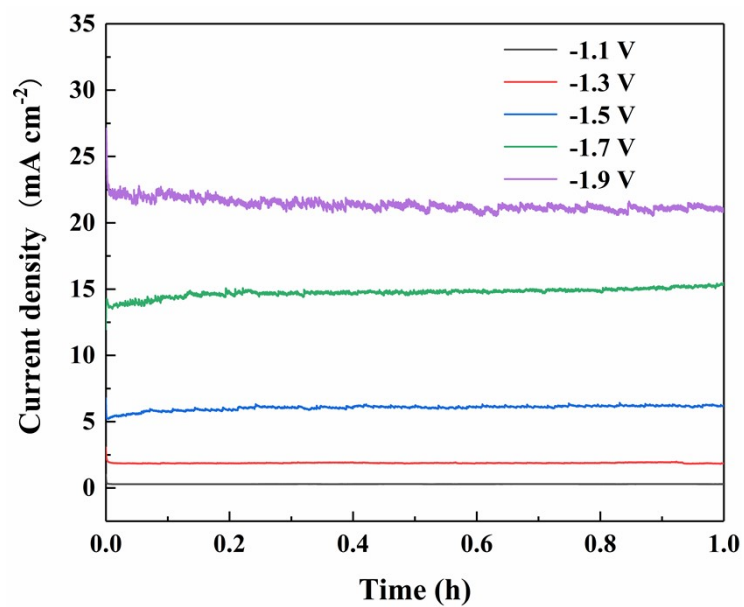


**Fig. S15** I-t curves of individual ECO<sub>2</sub>RR with TBP-CoPc/CNTs at different potentials (V vs. Ag/AgCl).

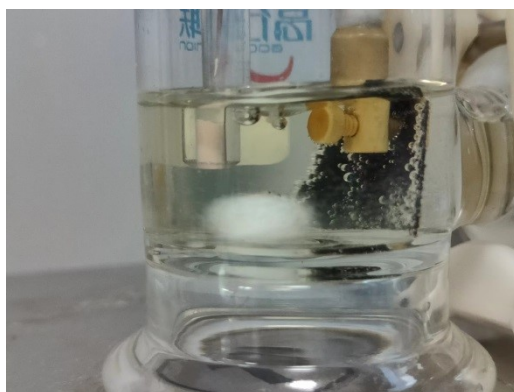


**Fig. S16** The optical photograph at the anodic part of H-cell after CPE for HMFOR at 1.0 V

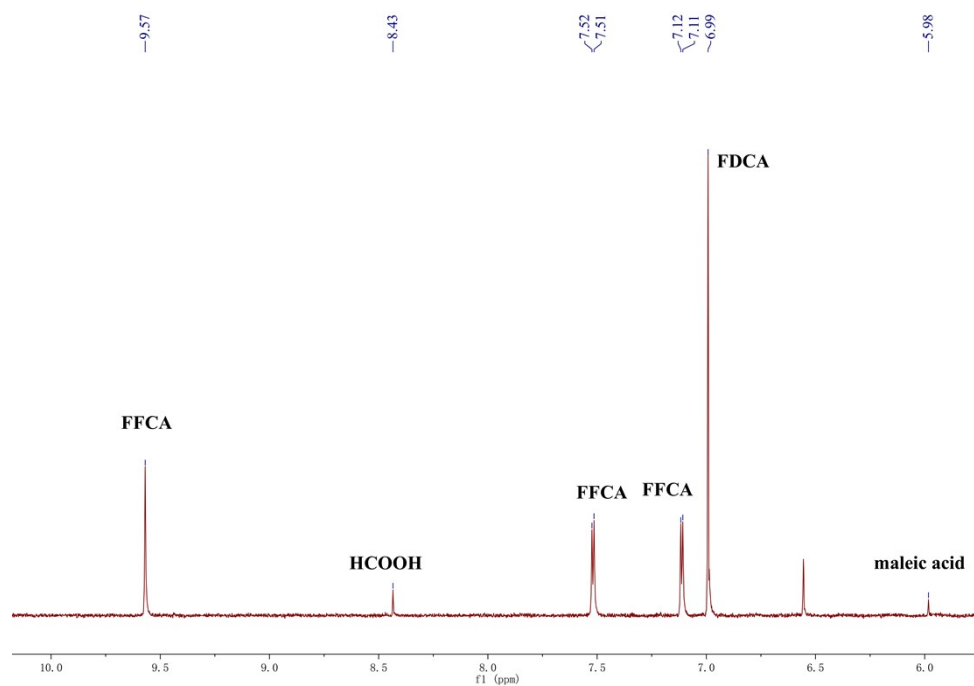


Fig. S17  $^1\text{H}$  NMR spectrum of anolyte after CPE for HMFOR at 1.0 V

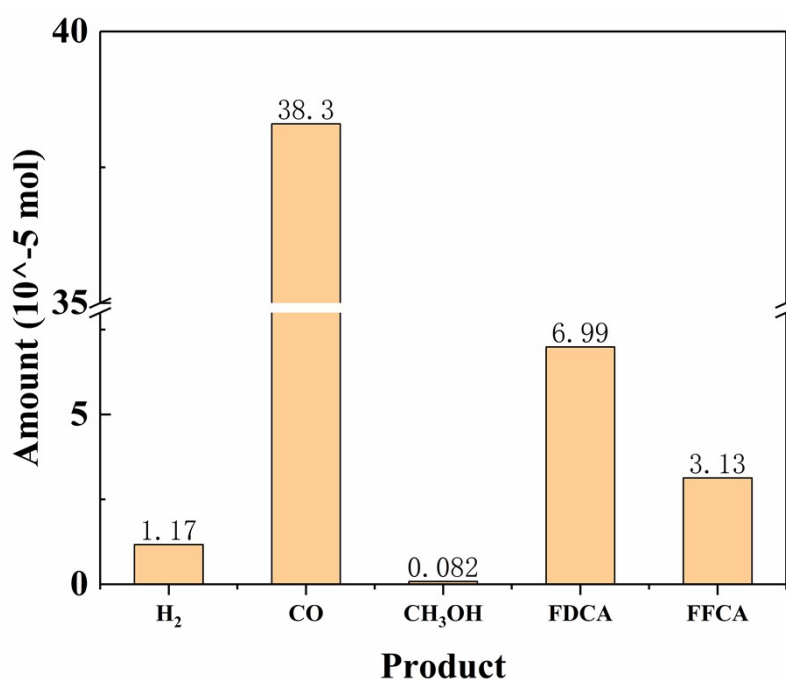


Fig. S18 Product distribution in the sun-light-driven paired electrolysis.

### 3. Reference

1. L. Luan, W. Fang, W. Liu, M. Tian, Y. Ni, X. Chen, X. Yu, J. He, Y. Yang and X. Li, *J. Porphyrins Phthalocyanines*, 2016, **20**, 397-406.

2. I. M. Denekamp, F. L. P. Veenstra, P. Jungbacker and G. Rothenberg, *Appl. Organomet. Chem.*, 2019, **33**, e4872.
3. A. Das and S. S. Stahl, *Angew. Chem. Int. Ed.*, 2017, **56**, 8892-8897.
4. M. J. Frisch, *et al. Gaussian 09, revision D.01 (Gaussian, 2009)*.